JOURNAL OF CATALYSIS 87, 163–178 (1984)

Spectroscopic and Catalytic Study on Metal Carbonyl Clusters Supported on Cab-O-Sil

I. Impregnation and Decomposition of $Fe_3(CO)_{12}$

K. LÁZÁR,* K. MATUSEK,* J. MINK,* S. DOBOS,* L. GUCZI,*,[1] A. VIZI-OROSZ,† L. MARKÓ,† AND W. M. REIFF‡

*Institute of Isotopes of the Hungarian Academy of Sciences, P.O. Box 77, H-1525 Budapest, and †Department of Organic Chemistry, Veszprém University, H-8200 Veszprém, Hungary; and ‡Department of Chemistry, Northeastern University, Boston, Massachusetts 02115

Received September 9, 1982; revised July 7, 1983

Impregnation of $Fe_3(CO)_{12}$ on Cab-O-Sil has been studied by ir spectroscopy, Mössbauer spectroscopy, and mass spectrometry. Isotope exchange between CO ligands of the impregnated sample and gas phase CO molecules was also investigated. On impregnation, two types of interaction can be distinguished: (i) interaction of the type Fe—C≡O···HO—Si and $\rangle$C=O···HO—Si, shown by the shift to lower and higher ir frequencies for bridged and for terminal CO, respectively, and (ii) interaction between the metal framework and the support revealed in the oxidation of iron to form very small iron oxide particles. On impregnation a small amount of CO is evolved as a result of the interaction. CO exchange occurs faster with alumina-supported clusters than with silica-supported samples. On decomposition up to 370 K, the metal framework is retained and the cluster structure can be partly restored in a CO atmosphere. Above 420 K, $Fe_3(CO)_{12}$ is decomposed to form Fe^{2+} oxide on the surface. A possible mechanism for impregnation is discussed in terms of electron donation from the support oxygen to the iron *d*-bands as a result of which the metal–carbon bond strength is influenced. On decomposition the metallic iron interacts with the support OH groups causing oxidation and Fe^{2+} formation.

INTRODUCTION

Application of metal carbonyl clusters (MCC) for preparation of highly dispersed metal catalysts on various supports was introduced several years ago (*1–4*). In comparison with other methods of preparation, such as impregnation of a support with an aqueous solution of an inorganic salt, this method gives superior metal dispersion (*5*) and outstanding specific activity (*6, 7*). Furthermore, by using bimetallic clusters, bimetallic catalysts can be produced for those metal combinations where the reducibility of one or both metals is difficult (*8*).

Due to the very small size of the resulting metal particles, stability of a MCC-prepared catalyst is one of the most important problems. By choosing the appropriate oxide as a carrier, small metal particles can be stabilized. However, too weak or too strong an interaction tends to agglomerate the metallic particles or to oxidize part of the zero-valent metal atoms after decomposition, respectively. Although we have obtained a large amount of information about the decomposition of supported MCC (*6, 9*), few data are available on the interaction between the support and the MCC during decomposition (*2, 10*).

Another factor that seriously influences the catalytic activity is the ambient atmosphere in which the decomposition takes place. The catalyst prepared from MCC upon decomposition in He revealed very high activity in CO hydrogenation and in *n*-butane hydrogenolysis (*6, 7*). This was explained by the presence of highly dispersed carbon captured in the metallic framework, thereby stabilizing the individual metal ag-

[1] To whom correspondence should be addressed.

0021-9517/84 $3.00

gregates. The presence of carbon has been proved in the case of the decomposition of osmium carbonyl clusters (*11*).

The decomposition of supported iron clusters has been studied for $Fe(CO)_5$, $Fe_2(CO)_9$, and $Fe_3(CO)_{12}$ supported on γ-Al_2O_3, by both temperature-programmed decomposition and ir spectroscopy, demonstrating in detail the presence of reversibly formed subcarbonyl species (*10*). High temperature heating as well as oxidation–reduction cycles lowered the metal dispersion to a large extent (*5*). Formation of $[HFe_3(CO)_{11}]^-$-ion was reported as a product of interaction of alumina and magnesia with $Fe(CO)_5$ and $Fe_3(CO)_{12}$ dissolved in hexane (*12*). The influence of water content and surface hydroxyl groups of alumina and magnesia supports on the properties of the catalyst formed was investigated by ferromagnetic resonance. The Mössbauer spectrum of a decomposed carbonyl on magnesia was also reported (*13*). Reversibly formed carbonyls are also observed on Na-Y zeolites (*14*), whereas silica was considered not to stabilize subcarbonyl species (*10, 12*).

In the present work investigations were focused on the interaction developed between the metal carbonyl cluster and Cab-O-Sil at deposition under exactly the same conditions as have been applied for the preparation of supported iron, ruthenium and iron–ruthenium catalysts used in kinetic studies of catalysis (*6, 7, 9, 15–17*). The stability of the surface complexes and thermal treatment in different atmospheres, below 400 K, has been studied. Since the active metallic phase is being developed during decomposition of supported metal carbonyl cluster in the temperature range between 400 and 770 K, its mechanism and the role of carbon deposited in this decomposition were also studied.

In this paper (Part I) work on $Fe_3(CO)_{12}$ deposited on Cab-O-Sil will be reported, and in Part II that on $Ru_3(CO)_{12}$ and on $Ru_3(CO)_{12}$ + $Fe_3(CO)_{12}$ will be presented.

EXPERIMENTAL

Materials. Silica gel (SAS 50–100 mesh, specific surface area 580 m^2/g pore volume 0.23 ml), Cab-O-Sil HS 5 (Cabot Co., Boston, Mass.), and gamma-alumina (Woelm, No. 1424) have been used as supports.

$Fe_3(CO)_{12}$ was purchased from Strem Chemicals. A new method was developed for the synthesis of ^{57}Fe-labeled $Fe_3(CO)_{12}$, as follows:

$$^{57}Fe(\text{metal}) \xrightarrow[\text{at 450 K in a sealed tube}]{+I_2} {}^{57}FeI_2 \xrightarrow[\text{100 bar autoclave, 4 days at 350 and 390 K}]{NH_4OH,CO:H_2 = 1:1} {}^{57}Fe(CO)_5$$

$$^{57}Fe(CO)_5 \xrightarrow{+KOH} [{}^{57}Fe(CO)_4]^{2-} \xrightarrow[\text{then } H^+]{\text{first oxidation}} {}^{57}Fe_3(CO)_{12}$$

^{57}Fe-labeled $Fe_3(CO)_{12}$, enriched to 90%, was used for Mössbauer spectroscopy.

Water species were carefully removed from hexane by storage on freshly dried $CaCl_2$ and metallic sodium for 24 h, then by distillation from $LiAlH_4$. Finally, the hexane was stored in the presence of metallic sodium.

^{13}CO was purchased from the USSR.

The supported carbonyl cluster samples were prepared in the following way. The support was first evacuated at 570 K overnight to 10^{-3} Pa. $Fe_3(CO)_{12}$ was dissolved in hexane and carefully deoxygenated. After contacting the solution with the support, hexane was frozen-out and the impregnated sample was evacuated at room temperature overnight. Metal loading was normally 1 wt% as measured by x-ray fluorescence. The transfer of the impregnated samples into the Mössbauer and ir cells was carried out under purified nitrogen.

The gases used were purified by removing traces of oxygen with manganous oxide followed by passing through molecular sieves. Hydrogen was purified by contact with a BASF 11 deoxygenator followed by a molecular sieve unit.

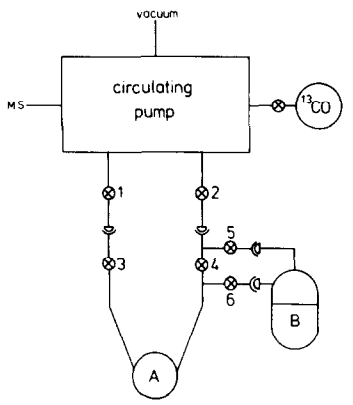

FIG. 1. Experimental setup for measuring CO evolution during the impregnation of support with MCC. A, reaction vessel (56.9 ml) for SiO_2, Al_2O_3; B, glass vessel for hexane solution; (1–6): Porasil valves with Viton ring.

Apparatus. A mass spectrometer (Kratos MS 10 C2) was used to measure the CO evolution and the molecular exchange of CO in the supported cluster. The *in situ* impregnation apparatus, connected to the mass spectrometer via a capillary leak, is shown in Fig. 1. The procedure was as follows. A 0.3 g support was put into A and was evacuated overnight at different temperatures. $Fe_3(CO)_{12}$ dissolved in hexane was put into B, frozen at liquid nitrogen temperature and evacuated with valves 3 and 4 closed. The freezing–pumping cycle was repeated three times. With all valves closed the lower part was detached at the hemispherical joints and the hexane solution was brought into contact with the support via valve 6. After shaking for about 5 min, hexane was transferred back to B by freezing at liquid nitrogen temperature. Any CO evolved remained in the gas phase. After reconnection of the apparatus to the circulating system (circulating rate 5 ml/s), valves 1 and 2 were opened for evacuation and then the system was filled up with the CO evolved during the deposition of $Fe_3(CO)_{12}$, via valves 3, 5, and 6 (valve 4 remained closed). During this procedure hexane in B was kept frozen. The system was filled with helium to 8 kPa and the amount of CO was measured by MS. At constant pressure the MS signal is proportional to the amount of CO to within 2%.

The exchange between CO molecules in the supported cluster and in the gas phase was followed by ^{13}CO and measured in the same apparatus. After the exchange was accomplished, $Fe_3(CO)_{12}$ was decomposed by heating the sample to 770 K (heating rate of 20 K min^{-1}).

Mössbauer spectra were obtained in the constant acceleration mode by a Mössbauer spectrometer and ICA-70 multichannel analyzer. Evaluation of spectra was performed by a Sirius-40 program set (*18*). A single line $^{57}Co/Cr$ source was used. Isomer shift values are related to metallic iron.

For the Mössbauer measurements a new cell was designed. In the cell it was possible to carry out *in situ* measurements and heat treatments in different atmospheres. The sample was studied between 80 and 800 K without exposure to air. A sketch of the cell is presented in Fig. 2. Measurements were carried out also at a temperature of 1.6 K.

In the evaluation of the Mössbauer spectra, the influence of texture and the Goldansky–Kariagin effect were not taken into account. The differences in the recoil-free fraction of the Mössbauer effect of the various components were neglected.

Infrared spectra were measured on a Digilab FTS-14 interferometer equipped with a Nova-1200 computer. Spectra were recorded by collecting and signal averaging 200 scans with a resolution of 4 cm^{-1}. The single spectra were stored on the disk, while the double beam spectra were referenced against the Cab-O-Sil spectrum. The infrared cell, detailed elsewhere (*19*), was made of Pyrex glass with a quartz tube heater. The sample pellet was pressed into a 25-mm-diameter wafer. The cell could be evacuated to 5×10^{-2} Pa and the pressure of the added gases was measured by a Datametrics Electronic manometer.

In some cases, a conventional TPD appa-

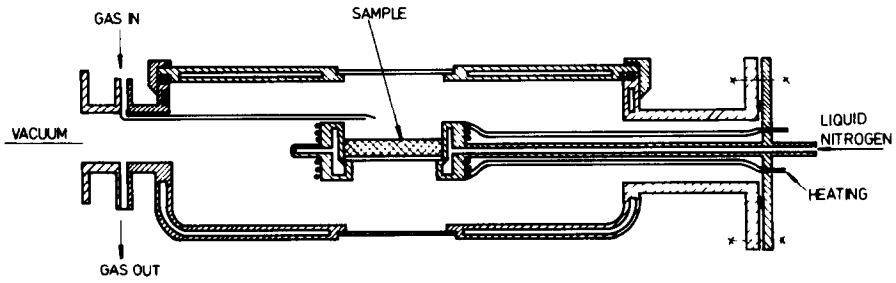

FIG. 2. Mössbauer cell for *in situ* measurements.

ratus was used in the flow system (*6*) with a temperature programmer (Chinoin LP 839).

RESULTS

Impregnation

Evolution of CO molecules during impregnation in vacuum was measured on Cab-O-Sil and on silica gel. The detected signal of $m/e = 28$ corresponds to 0.2 molecules CO evolved per molecule of $Fe_3(CO)_{12}$. The concentration dependence of impregnation was also studied. Clusters from solutions which correspond to 1 wt% metal loading were not adsorbed totally: a small amount remained in the solvent. No other differences were observed between samples of 0.1, 0.3, and 1.0 wt% metal loading in the course of the further steps. Although the use of an alumina support is not the subject of the present study, for the sake of comparison the impregnation of $Fe_3(CO)_{12}$ was also measured on it. Here one molecule CO per $Fe_3(CO)_{12}$ molecule was evolved.

In order to obtain deeper insight into the nature of the interaction between the support and $Fe_3(CO)_{12}$, ir-, and Mössbauer measurements were also carried out. Ir spectra of $Fe_3(CO)_{12}$ in hexane solution along with iron dodecacarbonyl supported on Cab-O-Sil were recorded and are shown in Fig. 3. Although the cluster concentration on the support as normally prepared is so low that the presence of the cluster in crystalline form can be neglected, for better comparison the spectra of $Fe_3(CO)_{12}$ in KBr and in Nujol were taken. These are presented in Fig. 3. All the data are summarized in Table 1, and the spectra of $Fe_3(CO)_{12}$ in a N_2 matrix at 20 K (*20*) and on NaY zeolite (*14*) are also presented.

On impregnation all bands are broadened in comparison with the spectra recorded in hexane solution. It is well known that $Fe_3(CO)_{12}$ has different structures in solution and in the solid crystalline state (*21*). However, the terminal CO stretching frequency in the impregnated state is higher than in any other structures except those

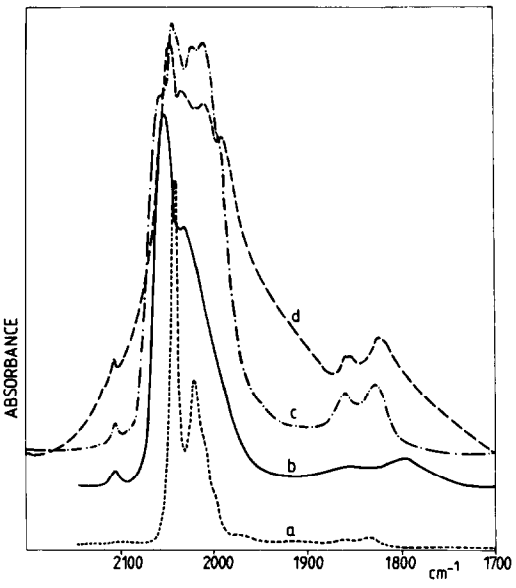

FIG. 3. Infrared spectra of $Fe_3(CO)_{12}$. (a) In hexane solution, (b) supported on Cab-O-Sil, (c) crystalline in KBr, (d) crystalline in Nujol.

TABLE 1

Carbonyl Stretching Frequencies (cm^{-1})

$Fe_3(CO)_{12}$ in hexane solution	$Fe_3(CO)_{12}$ in KBr pellet	$Fe_3(CO)_{12}$ in Nujol	$Fe_3(CO)_{12}$ in N_2 matrix (Ref. (*20*))	$Fe_3(CO)_{12}$ on NaY zeolite (Ref. (*14*))	$Fe_3(CO)_{12}$ on Cab-O-Sil	Assignments
2103 vw	2107 vw	2107 vw	2112 vw	2112 mw	2113 vw	
2085 vw	2060 sh	2052 vs	2058 vs	2060 s	2060 vvs	
2048 vvs	2048 vs		2053 vs			
2025 s		2038 s	2036 s	2045 s	2038 vs	
	2028 s		2029 sh			Terminal
2015 sh	2015 s	2015 s	2021 w			CO
			2014 w	2025 s	2015 sh	
			2010 m			
2002 vw			2004 vw			
	1995 sh	1995 s		1995 s		
				1965 s		
1970 vw,b				1945 s		
			1867 w			
1868 w	1862 m	1857 m	1862 w		1869 w,b	
1842 vw,b	1830 m	1825 m	1829 m			Bridged
1833 w,b			1827 m	1800 mv	1805 wb	CO
				1770 m		

observed in matrix isolation and in zeolite supported systems. The bridged carbonyl bands were shifted to a larger extent and in the opposite direction. As Fig. 3 shows, there is also an increase in the intensities. One band (at 1869 cm^{-1}) was not affected by the cluster–support interaction, whereas the other two bands (1842 and 1833 cm^{-1}) were replaced by a band at 1805 cm^{-1} (see Table 1).

Mössbauer spectra of the impregnated samples were measured at 80 K and are shown in Fig. 4A. The spectrum of the 1.5 wt% sample (curve b) resembles that of $Fe_3(CO)_{12}$ dissolved in hexane (curve a) and can be represented as the sum of the spectrum of the unchanged $Fe_3(CO)_{12}$ (69%) and that of another component to be discussed later. The spectrum of the 0.7 wt% sample (curve c) is a doublet with 12% asymmetry. This spectrum also can be deconvoluted to that of $Fe_3(CO)_{12}$ (14%) and the other component to be described later. The spectrum of the 0.4 wt% sample (curve d) apparently shows no unchanged $Fe_3(CO)_{12}$ cluster. The data are presented in Table 2.

The 0.4 wt% sample was also measured at 1.6 K. The spectrum (Fig. 4B) at this temperature clearly resolved two compo-

TABLE 2

Change of the Mössbauer Parameters of $Fe_3(CO)_{12}$ by Impregnation on Cab-O-Sil

	Original component	In contact with support	$\frac{\chi^2}{\langle\chi^2\rangle}$	Sample
IS_1	0.01	—		
IS_2	0.11	—	1.04	Crystalline
QS	1.08	—		
IS_1	0.05	—		
IS_2	0.11	—	2.66	In hexane
QS	1.11	—		solution
IS_1	0.09	—		
IS_2	0.12	0.41	1.11	1.5 wt%
QS	1.11	1.01		impregnated
Ratio[a]	0.69	0.31		
IS_1	0.18	—		
IS_2	0.16	0.45	1.43	0.7 wt%
QS	1.10	0.94		impregnated
Ratio[a]	0.14	0.86		
IS_2	—	0.43	1.50	0.4 wt%
QS	—	0.95		impregnated

Note. IS_1 is the isomer shift value of the inner peak, and IS_2 is that of the outer doublet. QS is the quadrupole splitting. Values are in mm s^{-1}. $\chi^2/\langle\chi^2\rangle$ characterizes the quality of fitting, its optimal value being between 1 and 2.

[a] Relative intensities of the two components.

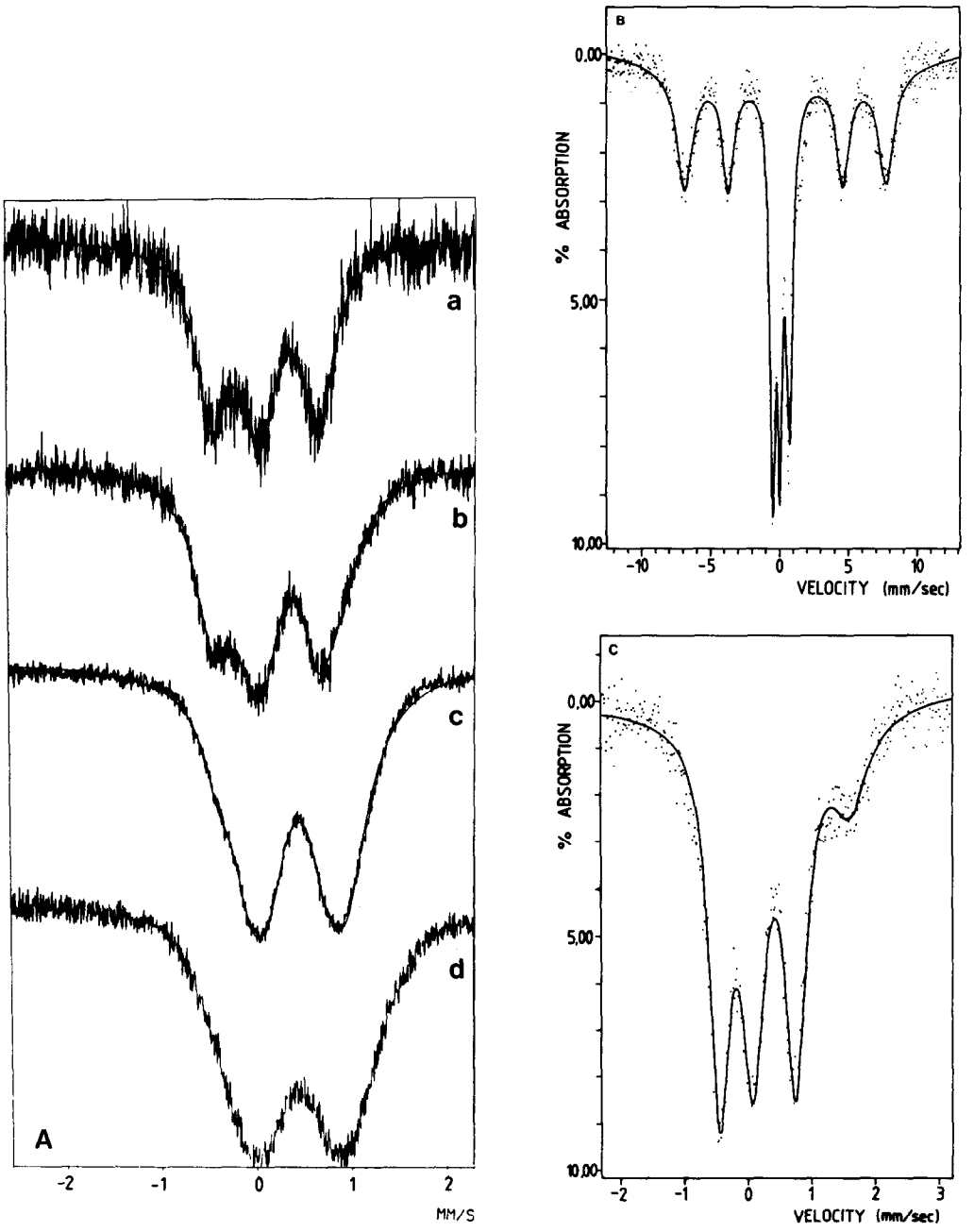

FIG. 4. (A) Mössbauer spectra at 80 K of $Fe_3(CO)_{12}$. (a) In hexane solution, (b) impregnated on Cab-O-Sil, 1.5 wt% metal, (c) impregnated on Cab-O-Sil, 0.7 wt% metal, (d) impregnated on Cab-O-Sil, 0.4 wt% metal. (B) Mössbauer spectra at 1.6 K of $Fe(CO)_{12}$ impregnated on Cab-O-Sil, 0.4 wt% metal. (C) Mössbauer spectra at 1.6 K of impregnated $Fe_3(CO)_{12}$ (reference spectrum). The fourth broad peak at the right-hand side belongs to the magnetically split component.

TABLE 3

Influence of the Temperature and the Pretreatment of the Support on the Rate of Exchange and on the Fixation of Fe–MCC Clusters

Support	Pretreatment temperature (K)	Temperature of measurement (K)	Amount of CO on support (mol × 10^6)	$\frac{^{12}CO}{^{12}CO + {}^{13}CO}$	Rate of exchange (mol s^{-1} 10^{-5})	$\frac{^{12}CO_s/^{12}CO_t}{\Sigma CO_s/\Sigma CO_t}$[a]	Percentage of CO not recovered from the cluster
SiO_2	400	350	99.0	0.59	0.35	1.00	12.0
	570	350	99.4	0.55	1.04	1.02	14.3
	770	350	89.5	0.59	1.08	0.98	6.4
Al_2O_3	400	275	96.5	0.60	0.05	1.15	20.7
	570	275	91.3	0.56	0.37	1.11	23.0
	770	275	79.1	0.54	0.43	1.06	40.0
Al_2O_3	570	275	85.3	0.53	0.36	1.38	38.1
	570	315	91.8	0.48	0.85	1.23	36.3
	570	350	88.5	0.37	1.68	1.19	24.3

Note. CO is defined as the sum of the quantities of ^{12}CO and ^{13}CO; CO_s and CO_t refer to the quantity of CO on the support and to the total CO quantity on the support and in the gas phase.

[a] At complete isotope equilibrium this value should be 1.

nents. The first has the three transitions of the original $Fe_3(CO)_{12}$ (middle part of Fig. 4B measured at lower velocity is plotted in Fig. 4C) with the parameters $IS_1 = 0.08$ mm s^{-1}, $IS_2 = 0.15$ mm s^{-1}, and $QS = 1.19$ mm s^{-1}. The second component has a line separation corresponding to an internal 454 kOe magnetic field with $IS = 0.45$ mm s^{-1}, clearly indicative of high spin Fe^{3+} and substantial oxidation of $Fe_3(CO)_{12}$ on the support. In Fig. 4B the ratio of the area of unchanged $Fe_3(CO)_{12}$ to the total area of the spectrum is 37%.

The rate of isotope exchange between CO molecules in the supported $Fe_3(CO)_{12}$ and ^{13}CO in the gas phase gives an indication of the bond strength of CO ligands to the metal framework. If strong interaction exists between the support and the cluster after impregnation, CO ligands might be activated and their exchange is facilitated. The data are presented in Table 3. The exchange on alumina-supported $Fe_3(CO)_{12}$ is faster than for the silica-supported cluster because the same range of exchange rate can only be achieved on silica by going to a higher temperature of measurement. The rate is higher at higher pretreatment temperature. The last columns show the "extent" of the exchange at a particular temperature. If there is complete isotope equilibrium, the ratio in column 7 should be 1, as is the case on silica-supported $Fe_3(CO)_{12}$. The ratio deviates considerably from unity on alumina-supported cluster which indicates that not all CO ligands participate in the exchange process. As the temperature is increased, the extent of exchange increases even on alumina, but here the temperature is close to the lower limit of the cluster decomposition temperature.

Thermal Decomposition

Decomposition of $Fe_3(CO)_{12}$ impregnated samples was first measured up to 400 K in He. CO signals observed in the mass spectrometer ($m/e = 28$) are presented in Fig. 5. Instead of a sharp single peak characteristic of the crystalline form, the decomposition of the supported clusters shows a broadened peak which is reminiscent of the broad bands observed in ir spectra of the supported clusters. This is entirely due to the different environments of the cluster as a consequence of the activated state after deposition. Hydrogen evolution was also observed on decomposition and will be discussed in Part II. The amount of CO recovered on decomposition depends on the pre-

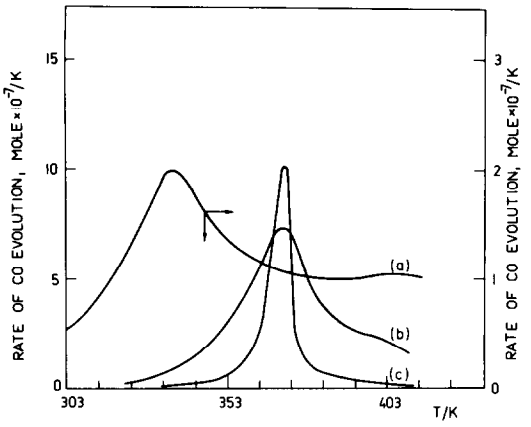

FIG. 5. TPDC curves for $Fe_3(CO)_{12}$. (a) Supported on Al_2O_3 pretreated at 570 K, (b) supported on Cab-O-Sil pretreated at 570 K, (c) crystalline $Fe_3(CO)_{12}$.

treatment temperature as indicated in Table 4.

As already shown in the exchange reactions, the cluster is in a more activated state on alumina than on Cab-O-Sil. As a consequence, the maximum is shifted to lower temperature in comparison to Cab-O-Sil. On the other hand, less CO could be recovered during decomposition on alumina than on Cab-O-Sil.

Thermal decomposition was also followed by infrared spectroscopy. The spectra for the $Fe_3(CO)_{12}$/Cab-O-Sil sample decomposed in H_2 and measured at different temperatures are presented in Fig. 6. A substantial part of the cluster has decomposed below 360 K, especially between 301 and 341 K where the decomposition is very fast and the relative intensity of terminal CO bands is also changed. In Fig. 7 it is demonstrated that at 361 K, the spectrum that is characteristic of the original cluster has disappeared, and with increasing temperature the bands are shifted toward lower wavenumbers. In the high temperature range the spectrum resembles that of adsorbed CO. Thus, at 381 K the bands at 2020 and 2000 cm^{-1} may be assigned to CO resulting from the original cluster during the decomposition and adsorbed on the metallic part formed after decomposition.

When decomposition is carried out in

TABLE 4

Decomposition of $Fe_3(CO)_{12}$ Supported on Cab-O-Sil and on Alumina

Support	Pretreatment temperature (K)	Amount of CO (mol × 10^5)	
		In $Fe_3(CO)_{12}$ impregnated	After decomposition to 470 K
Cab-O-Sil	570	3.1	2.9
Cab-O-Sil	770	3.3	2.5
γ-Al_2O_3	570	3.15	1.9

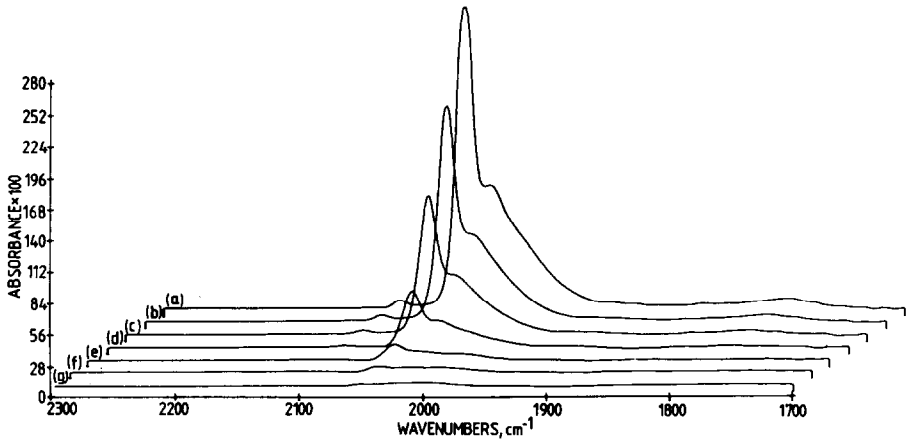

FIG. 6. Three-dimensional plot of thermal decomposition for $Fe_3(CO)_{12}$/Cab-O-Sil under stream of H_2 (a) 301 K; (b) 311 K; (c) 321 K; (d) 331 K; (e) 341 K; (f) 351 K; (g) 361 K.

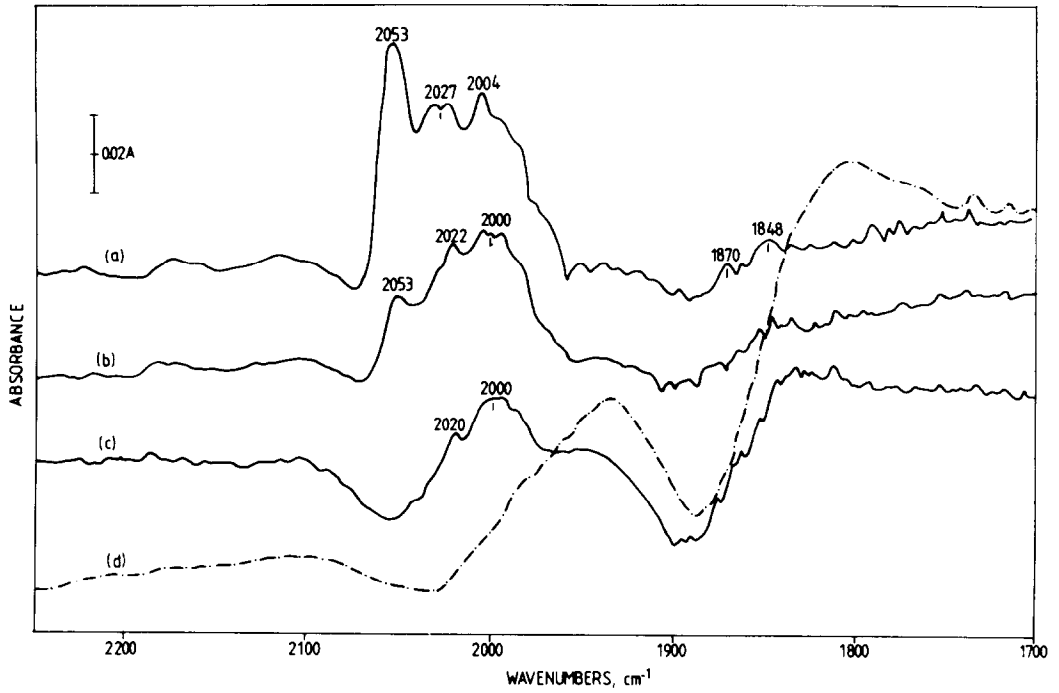

FIG. 7. Thermal decomposition of $Fe_3(CO)_{12}$/Cab-O-Sil at higher temperature under stream of H_2 (a) 351 K; (b) 361 K; (c) 381 K; (d) after full decomposition the SiO_2 spectrum at 683 K against the cooled sample at 303 K.

vacuum the spectra are similar to those shown in Fig. 6. The only difference is that decomposition here is slower than in hydrogen.

Decomposition can be quantitatively characterized by the decrease of the most intense terminal CO stretching band characteristic of CO in the cluster. Figure 8 presents the relative intensity of the band at 2060 cm^{-1} vs temperature. Between 330 and 340 K, decomposition is fast. This band disappears faster for the cluster decomposed in hydrogen than for that treated under vacuum.

A broad band at 1850 cm^{-1} has been observed at 350 K, but with a further rise in temperature the intensity of this band attenuated.

CO adsorption at 300 K in the presence of 1 kPa CO gas on a sample which had been decomposed up to 700 K could not be observed.

An interesting feature is shown by studying the solid phase by Mössbauer spectroscopy after decomposition. Mössbauer spectra of the impregnated and subsequently decomposed $Fe_3(CO)_{12}$ on Cab-O-Sil sam-

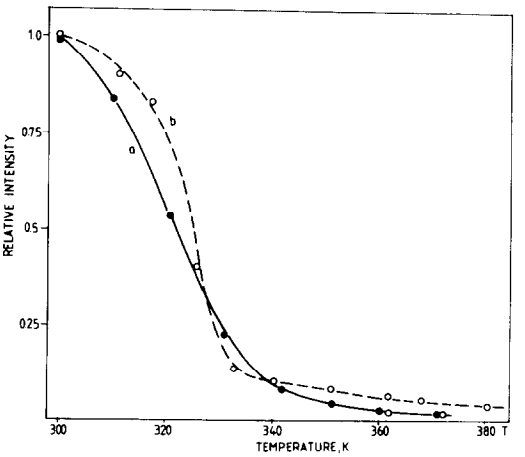

FIG. 8. Temperature dependence of relative band intensity at 2060 cm^{-1} for $Fe_3(CO)_{12}$/Cab-O-Sil. (a) Decomposition under H_2, (b) decomposition under vacuum.

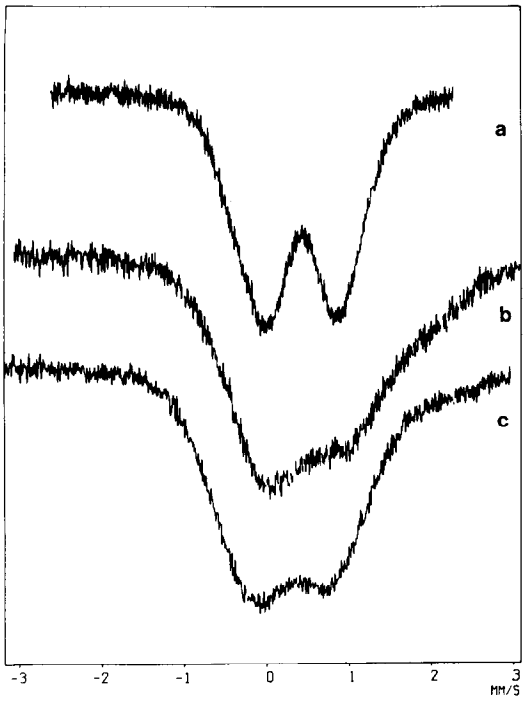

FIG. 9. Mössbauer spectra of decomposed $Fe_3(CO)_{12}$ taken at 80 K. (a) After impregnation (see Figure 4(d)), (b) heated in vacuum at 370 K, (c) sample (b) exposed to CO at 370 K.

ples were recorded during and after heat treatments carried out in H_2 and He at 370, 420, 470, 570, and 720 K.

Decomposition below 370 K in hydrogen and helium gave similar results: symmetric doublets were recorded with IS = 0.43 mm s^{-1} and QS = 1.08 mm s^{-1} values.

The behavior of samples decomposing in vacuum was entirely different (see Fig. 9). After treatment at 370 K, a sum of broad lines could be recorded. Readsorption of CO considerably affected the shape of the spectra and a part of the initial doublet was restored.

Mössbauer spectra of the sample treated in hydrogen at 420 K for 2 h show Fe^{2+} and Fe^{3+} components recorded at 80 K. Leaving this sample at room temperature the Fe^{2+} component slowly disappeared and only high spin ferric ions were present due to the interaction of iron with the support surface. Repeated reduction at 720 K for 1 h restored the original Fe^{2+}/Fe^{3+} ratio recorded after decomposition at 420 K but the IS value of the Fe^{3+} component was significantly higher than after the original treatment at 420 K. After 24 h the spectrum showed a smaller IS value for Fe^{3+} and the proportion of this component was higher than previously (see Fig. 10 and Table 5). This phenomenon, i.e., the change of the IS

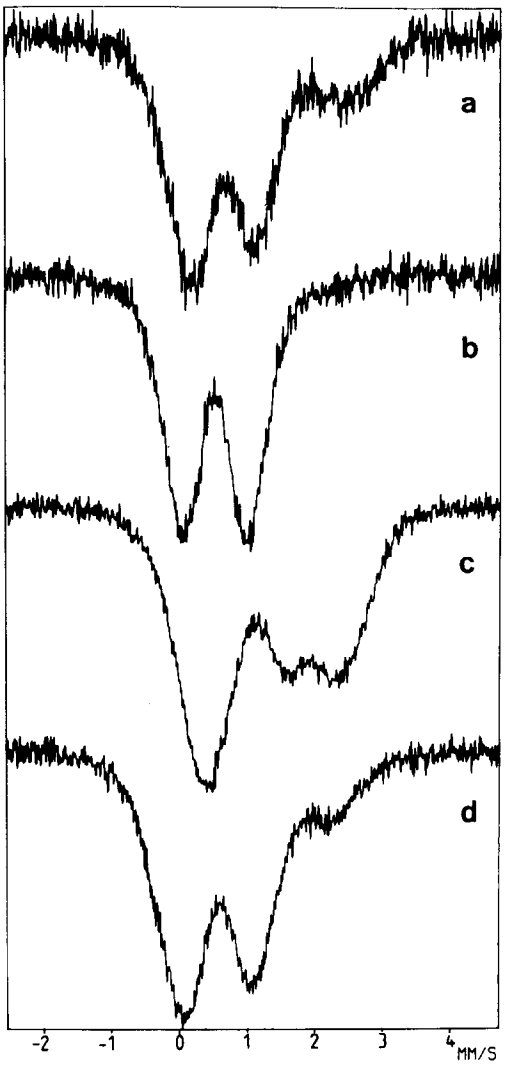

FIG. 10. Mössbauer spectra of 0.4 wt% iron containing samples after treatments in hydrogen. (a) Treatment at 420 K, measured at 80 K, (b) after staying at 300 K, measured at 300 K, (c) treatment at 720 K, measured at 80 K, (d) after staying at 300 K, measured at 300 K.

TABLE 5

Mössbauer Parameters after Hydrogen Treatments at 420 and 720 K

Temperature of heat treatment (K)	Component	Temperature of measurement (K)							
		80				300			
		IS (mm s^{-1})	*QS* (mm s^{-1})	*R*	$\frac{\chi^2}{\langle\chi^2\rangle}$	*IS* (mm s^{-1})	*QS* (mm s^{-1})	*R*	$\frac{\chi^2}{\langle\chi^2\rangle}$
420	Fe^{2+}	1.05	2.50	26	1.14	—	—	—	1.19
	Fe^{3+}	0.47	0.92	74		0.32	0.97	100	
720	Fe^{2+}	1.36	1.95	57	1.95	1.06	2.10	20	1.99
	Fe^{3+}	0.79	1.20	43		0.34	1.12	80	

Note. *R* is the ratio of components in percent; the value of $\chi^2/\langle\chi^2\rangle$ characterizes the quality of the fit, its optimal value being between 1 and 2.

of Fe^{3+} from a high to a low value, could be repeated several times.

Hydrogen treatment for 24 h at 570 K yielded a ferromagnetic Fe^0 component in addition to Fe^{2+}, which amounts to about 14%. After 16 h, the partial oxidation of Fe^{2+} was also observed (see Fig. 11).

Samples were also investigated by x-ray diffraction. Most of them gave signals indicating the presence of very fine particles. After hydrogen treatment at 570 K, sharp peaks of iron (110) planes were detected with a plane distance of 0.202 nm. The estimated average diameter of the particles was 17 nm.

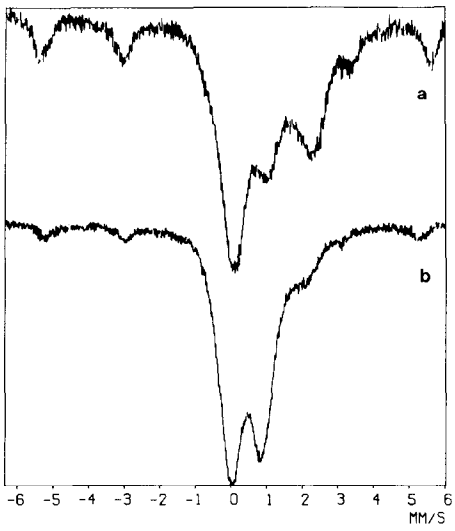

FIG. 11. Mössbauer spectra of 0.7 wt% iron containing sample in hydrogen. (a) After one-day treatment at 570 K, measured at 80 K, (b) sample (a) measured on the next day at 300 K.

Measurements were also carried out in helium. After treatment at 770 K for 15 min, a typical doublet could be observed at 80 K. The fitted parameters were *IS* = 1.07 mm s^{-1} and *QS* = 1.93 mm s^{-1}. After 24 h at room temperature, a greater part of the sample had also been oxidized and a high spin Fe^{3+} doublet was measured.

DISCUSSION

It has already been demonstrated that, in the genesis of highly dispersed, supported metal catalysts, the properties of the active metal are controlled by the very first step of the preparation, not only in the use of aqueous solutions of inorganic salts (*22*) but also in the case of metal organic substances (*23*). As we also indicated (*24*), neither too strong, nor too weak, interaction is required for the formation of active metal surfaces.

It is therefore important to examine the interaction between the support and the MCC in considering the preparation of dispersed metal catalysts. The discussion will

be confined to the properties of silica gel–MCC interaction, as the alumina–MCC system was studied just as a complementary one.

It is well known that, after the evacuation temperature applied here, structural OH groups are still present on silica gel (*25*). The reason why higher temperature was not used in the pretreatment of the support is that these OH groups may help the chemical bonding of the cluster during the impregnation.

Although silica gel is considered as one of the supports on which there is very weak interaction between the support and the impregnating species (*26*), the broadening of the ir- and Mössbauer spectra observed in the present work as well as the low temperature TPDC (temperature-programmed decomposition) curve suggest stronger than physical interaction between $Fe_3(CO)_{12}$ and Cab-O-Sil or even silica gel. This becomes clearer when the interaction between Al_2O_3 is compared with that on Cab-O-Sil (here we did not measure it in detail because it has been already discussed in Ref. (*10*)). Nevertheless, the exchange between CO molecules is faster on alumina, and CO evolution, which may be an indication of the "strength" of this interaction, is also higher on alumina. This is further supported by the marked change in the activation energy of the decomposition on alumina (see Fig. 5) while on Cab-O-Sil the broadening indicates no pronounced change in the activation energy. It is, however, an expected behavior and is a similar phenomenon to that found in the TPR spectra of, e.g., supported transition metal oxides (*27*).

Interaction between $Fe_3(CO)_{12}$ and Cab-O-Sil on impregnation can be interpreted from the Mössbauer data. Careful consideration of the Mössbauer spectra of samples with different cluster concentration (see Fig. 4 and Table 2) shows an overlapping of two spectra, one which is characteristic of the crystalline or molecular form of the cluster and the other with parameters of *IS* = 0.43 mm s^{-1} and *QS* = 0.95 mm s^{-1}. This *IS* value is too high to belong to zero-valent iron, but can be interpreted as a parameter of a partially oxidized component in accordance with the ir data in which a weak band above 2100 cm^{-1} might be an indication of the $Fe^{\delta+}$. The presence of $Fe_3(CO)_{12}$ in the original form is evidenced by the following arguments: (i) on impregnation nearly all CO ligands are retained on the metallic framework as measured by decomposition and indicated by the green color; (ii) some reversibility was detected at 370 K in vacuum and the subsequent CO treatment; (iii) treatment of the impregnated sample at 420 K gave an Fe^{2+} component (*29*) but supported Fe^{3+} ions can be reduced to Fe^{2+} only at high temperature (*30*); (iv) direct oxidation of our samples at 420 K gave a different *IS* value (0.38 mm s^{-1}) and a larger *QS* value (1.46 mm s^{-1}) and deconvolution of the spectra to Fe^{3+} with the parameters mentioned results in a maximum Fe^{3+} concentration of only 10%; (v) impregnated $Fe_3(CO)_{12}$ on the more basic MgO support gave only an Fe^{2+} component, besides Fe^0, after a treatment at 393 K (*13*). However, the spectra measured here at 80 K and those assigned to high spin Fe^{3+} in the iron–silica gel system (*28*) led us to assume the presence of high spin iron(III) ion and the Mössbauer measurements at 1.6 K indeed proved this idea. The value of the magnetic hyperfine field measured at 1.6 K (454 kOe) is less than that for α-Fe_2O_3 (515 kOe); it is closer to the values obtained for β- or γ-FeOOH (475 and 460 kOe, respectively). However, this component cannot be assigned to crystalline oxyhydroxides. The value of the internal hyperfine splitting for the present system does not change after high temperature treatments where the oxyhydroxides should undergo phase transitions.

The phenomenon observed could be interpreted by the interaction of iron and hydrogen, as was suggested by Davison *et al.* (*31*). On the other hand, the $[HFe_3(CO)_{11}]^-$ ion has been found when $Fe_3(CO)_{12}$ was

supported on MgO and Al_2O_3 supports. However, in our case the existence of this hydrido-carbonyl ion cannot be assumed because it has three lines and a smaller *IS* value in its Mössbauer spectra (*32*).

The most reasonable explanation is that in the first step interaction occurs between the OH groups on Cab-O-Sil and the bridged CO ligands in the cluster as illustrated by Scheme A.

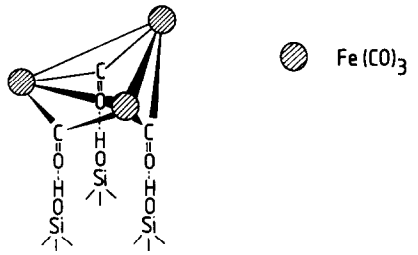

SCHEME A

In this way one can comprehend the shift of the bridged CO stretching frequency to lower wavenumbers which is a result of $\rangle C{=}O\cdots HO—$ coupling. Due to the electron shift inside the molecule the CO bond becomes stronger resulting in a shift of the terminal CO stretching frequencies to higher wavenumbers. Thus, the plane consisting of three iron atoms becomes parallel to the surface and stereochemically the oxygen atom in the $\rangle C{=}O\cdots HO—$ bond approaches the iron atom as illustrated in Scheme B.

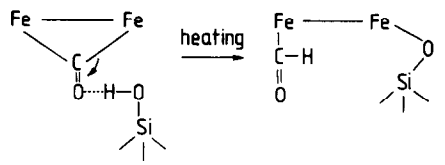

SCHEME B

Consequently, the formation of the Fe–O–Si bond eventually leads to the oxidation of iron, as was experienced. Similar bonding has been found in Rh–O–Si carbonyl derivatives (*33*) and the effect is similar to the support–cluster interaction observed in $Os_3(CO)_{12}$ and $Os_6(CO)_{18}$ clusters (*34*).

Furthermore, $Fe^{(0)}$ easily interacts with Si–OH groups and thus oxidation of $Fe^{(0)}$ takes place. The value of the hyperfine splitting (454 kOe) is, in fact, near to that of FeOOH and this may indicate the type of interaction. This oxidation is supported by the work of Burwell and co-workers (*35*) concerning the interaction of $Ni(CO)_4$ and OH groups in alumina. Oxidation of nickel easily occurs even in the presence of hydrogen.

As mentioned earlier, the catalytically active phase is developed during decomposition of the carbonyl cluster. However, this is, primarily influenced by the interaction at the impregnated stage. For example, if the interaction is strong, on decomposition part of the CO is retained on the surface in dissociated form such as oxide and carbide, which, in turn, strongly influences the properties of the catalyst formed (e.g., see Table 4, for Al_2O_3).

Treatment in vacuum at 370 K gave various components of more or less decomposed iron dodecacarbonyl molecules; the resultant Mössbauer spectrum is a broad asymmetric one indicating a distribution of iron environments. CO readsorption produces some homogeneity of fragments with somewhat greater symmetry in the Mössbauer spectrum.

Decomposition in hydrogen and in helium at 370 K produces more homogeneous and stable species. Their quadrupole splitting is 0.15 mm s^{-1} greater than that after impregnation, indicating the decrease of symmetry on heating. The isomer shift of products does not change appreciably, so no drastic oxidation has occurred. This can be correlated to the presence of carbon on the surface in the case of helium (*15*) and to hydrogen-iron interaction in the case of hydrogen as already discussed for the Fe/MgO system in hydrogen (*35*). Definite oxidation to the Fe^{2+} state takes place only above 420 K, as Mössbauer measurements show (*29*).

Infrared data give more information about the mechanism of the low tempera-

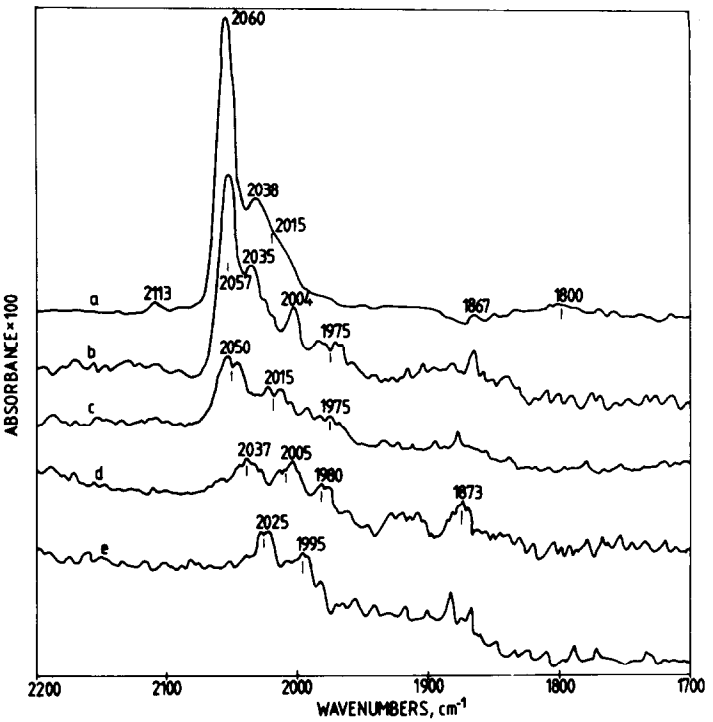

FIG. 12. Ratio spectra. (a) 331/341 K; (b) 351/361 K; (c) 361/371 K; (d) 381/391 K; (e) 391/401 K.

ture (<370 K) decomposition. At low temperature (up to 340 K) $Fe_3(CO)_{12}$ decomposes uniformly, i.e., the CO molecules leaving the clusters are equivalent. The ratio spectra (that is, the computed ratios of two spectra taken at two different temperatures) at lower temperatures are similar to the spectrum of the original $Fe_3(CO)_{12}$ on Cab-O-Sil (see Fig. 3b), as spectrum (a) shows in Fig. 12. At higher temperature (Fig. 12(b)) the bands at 2004 and 1975 cm^{-1} indicate that the mode of decomposition is changing. However, the band at about 2050 cm^{-1} in spectrum (c) still gives a faint indication of the presence of the original cluster. Spectra (d) and (e) resemble the spectra of chemisorbed CO molecules, i.e., by decreasing the coverage, the bands are continuously shifted to lower frequency (see, e.g., Ref. (*14*)). Furthermore, according to spectrum (d), with the appearance of adsorbed CO character, the very weak band at 1873 cm^{-1} can be assigned to the multiple-bonded CO. Above 401 K this band cannot be detected.

On low temperature decomposition, the metallic framework is not seriously distorted. This is shown by the reversible CO uptake as indicated by Mössbauer spectroscopy. Interaction between metal and support becomes even stronger when decomposition is continued above 400 K. Due to this interaction with the support, iron is oxidized mainly to Fe^{2+} (see Ref. (*14*)) but in some cases both Fe^{2+} and Fe^{3+} ions are present.

The possible reason for this low temperature oxidation during decomposition is the size of the small metal particles formed from the metallic framework after decomposition. Due to the lack of CO molecules, they are extremely unstable and can be stabilized by reacting with OH groups in Cab-O-Sil in the mechanism given by Dutartre *et al.* (*36*). Similar values have been also reported (*37, 38*) with the explanation of the

presence of highly distorted Fe^{3+} ions with very low symmetry. Considering that small metal loading on Cab-O-Sil may cause very strong interaction between iron and the support and, furthermore, that at small iron coverage Fe^{3+} ions are more or less individually bonded to the surface with highly distorted symmetry, this high *IS* value is acceptable. This explanation can be supported by the fact that after leaving the sample to stand for 24 h at room temperature the regular *IS* value can be measured, i.e., if time is available for surface rearrangement, a normal *IS* value for Fe^{3+} can be observed.

The next phenomenon to be discussed is the slow Fe^{2+} to Fe^{3+} oxidation at room temperature. This can be attributed to the reversibility of reduction similarly to that described on magnesia (*36*). It also means that interaction of the metal with the support is not very strong. Therefore, Fe^{2+} ions are not incorporated into the lattice of the support. Upon heating the $Fe_3(CO)_{12}$ on the support in helium up to 770 K, the main component is Fe^{2+} ion. This suggests that the oxidation process to Fe^{3+} is inhibited, and the Fe^{2+} component is somewhat more stable in this process. At room temperature, oxidation to Fe^{3+} takes place more slowly in comparison to that after hydrogen treatments. This phenomenon can be explained by the presence of carbon (*15*), which helps not only in the stabilization of small particles but in ensuring a reducing atmosphere in the environment of Fe^{2+} ions.

Long treatments in hydrogen at higher temperature result in the formation of large metal particles as shown in Fig. 11. This happens only for hydrogen-treated catalysts because here the carbon is hydrogenated off the surface and this results in an agglomeration of the small metal particles (*24*).

In conclusion, it has been established that, contrary to the literature data, interaction between $Fe_3(CO)_{12}$ and Cab-O-Sil exists at the impregnation stage via electron transfer. Decomposition below 370 K is more or less reversible, retaining the original metal framework, but at higher temperature formation of Fe^{2+} and Fe^{3+} occurs due to the interaction of metallic iron with the OH groups of the support. Formation of subcarbonyl species was not observed.

ACKNOWLEDGMENTS

The authors are indebted to Mrs. G. Stefler for preparation of the samples, to Mr. V. S. Alfeev (Novosibirsk) for TPD and impregnation measurements on Cab-O-Sil, to Mr. I. Bogyai for TPD measurements, and to Mrs. M. Klug for help in the ir measurements. The work was also sponsored by the NSF-DMR Solid State Chemistry Program (Grant DMR-8016441), and this assistance is gratefully acknowledged.

REFERENCES

1. Anderson, J. R., and Mainwaring, D. E., *J. Catal.* **35,** 162 (1974).
2. Anderson, J. R., Elmes, P. S., Howe, R. F., and Mainwaring, D. E., *J. Catal.* **50,** 518 (1978).
3. Basset, J. M., and Ugo, R., *in* "Aspects of Homogeneous Catalysis," (R. Ugo, Ed.), Vol. 3, p. 137 (1977). Reidel, Dordrecht, 1976.
4. Ugo, R., Psaro, R., Zanderighi, G. M., Basset, J. M., Theolier, A., and Smith, A. K., "Fundamental Research in Homogeneous Catalysis," Vol. 3, p. 579. Plenum, New York, 1979.
5. Brenner, A., *J. Chem. Soc. Chem. Commun.* 251 (1979).
6. Guczi, L., Schay, Z., Matusek, K., Bogyay, I., and Stefler, G., "Proceedings, 7th International Congress on Catalysis, (Tokyo, 1980)," p. 211, Kodansha/Elsevier, Tokyo/Amsterdam, 1981.
7. Schay, Z., and Guczi, L., *React. Kinet. Catal. Lett.* **14,** 207 (1980).
8. Guczi, L., Matusek, K., Manninger, I., Király, J., and Eszterle, M., "Preparation of Catalysts II," p. 391. Elsevier, Amsterdam, 1979.
9. Guczi, L., Schay, Z., Lázár, K., Vizi, A., and Markó, L., *Surf. Sci.* **106,** 516 (1981).
10. Brenner, A., and Hucul, D. A., *Inorg. Chem.* **18,** 2836 (1979).
11. Eady, C. R., Johnson, B. F. G., and Lewis, J., *J. Chem. Soc. Dalton* 2606 (1975).
12. Hugues, F., Smith, A. K., Ben Taarit, Y., Basset, J. M., Commereuc, D., and Chauvin, Y., *J. Chem. Soc. Chem. Commun.* 68 (1980).
13. Hugues, F., Bussière, P., Basset, J. M., Commereuc, D., Chauvin, Y., Bonneviot, L., and Olivier, D., "Proceedings, 7th International Congress on Catalysis (Tokyo 1980)," p. 418, Kodansha/Elsevier, Tokyo/Amsterdam, 1981.

14. Ballivet-Tkatchenko, D., Coudurier, G., Tkatchenko, I., and Figueiredo, C., *Prepr. Div. Pet. Chem. Amer. Chem. Soc.* **25,** 755 (1980).
15. Lázár, K., Schay, Z., and Guczi, L., *J. Mol. Catal.* **17,** 205 (1982).
16. Schay, Z., and Guczi, L., *Acta Chim. Acad. Sci. Hung.* **111,** 597 (1982).
17. Guczi, L., Schay, Z., and Bogyay, I., "Preparation of Catalysts III," p. 451. Elsevier, Amsterdam, 1983.
18. Kulcsár, K., Nagy, D. L., and Pócs, L., SIRIUS program system, KFKI report, **67** (1971).
19. Szilágyi, T., Sárkány, A., Mink, J., and Tétényi, P., *Acta Chim. Acad. Sci. Hung.* **101,** 259 (1979).
20. Poliakoff, M., and Turner, J. J., *J. Chem. Soc. (A)* **1971,** 654.
21. Nakamoto, K., "Infrared and Raman Spectra of Inorganic and Coordination Compounds." Wiley, New York, 1977.
22. Guczi, L., Matusek, K., Margitfalvi, J., Eszterle, M., and Till, F., *Acta Chim. Acad. Sci. Hung.* **101,** 107 (1979).
23. Guczi, L., Matusek, K., and Margitfalvi, J., *React. Kinet. Catal. Lett.* **8,** 309 (1978).
24. Guczi, L., *Catal. Rev. Sci. Eng.* **23,** 329 (1981).
25. Guczi, L., and Till, F., *Mater. Sci. Monographs,* No. 10, p. 908. Elsevier, Amsterdam, 1982.
26. Anderson, J. R., "Structure of Metallic Catalysts." Academic Press, New York, 1975.
27. Hurst, N. W., Gentry, S. J., Jones, A., and McNicol, B. D., *Catal. Rev. Sci. Eng.* **24,** 233 (1982).
28. Nagy, D. L., Dézsi, I., Eszterle, M., and Guczi, L., *J. Phys.* **40,** C2-78 (1979).
29. Schay, Z., Lázár, K., Mink, J., and Guczi, L., *J. Catal.* **87,** 179 (1984).
30. Berry, F. J., *Advan. Inorg. Chem. Radiochem.* **21,** 255 (1978).
31. Davison, A., McCleverty, J. A., and Wilkinson, G., *J. Chem. Soc.* 1133 (1963).
32. Greatrex, R., and Greenwood, N. N., *Discuss. Faraday Soc.* **47,** 126 (1969).
33. Vizi-Orosz, A., and Markó, L., *Transition Met. Chem.,* **7,** 216 (1982).
34. Collier, G., Hunt, D. J., Jackson, S. D., Moyes, R. B., Pickering, I. A., Wells, P. B., Simpson, A. F., and Whyman, R., *J. Catal.* **80,** 154 (1983).
35. Bjorklund, R. B., and Burwell, R. L., *J. Colloid Interf. Sci.* **70,** 383 (1979).
36. Dutartre, R., Bussière, P., Dalmon, J. A., and Martin, G. A., *J. Catal.* **59,** 382 (1979).
37. Berry, F. J., *Advan. Inorg. Chem. Radiochem.* **21,** 255 (1978).
38. Hobson, M. C., and Campbell, A. D., *J. Catal.* **8,** 294 (1967).